

AperTO - Archivio Istituzionale Open Access dell'Università di Torino

NO-donor thiocarbocyanines as multifunctional agents for Alzheimer's disease

This is the author's manuscript

Original Citation:

Availability:

This version is available <http://hdl.handle.net/2318/1522113> since 2015-12-22T11:25:25Z

Published version:

DOI:10.1016/j.bmc.2015.05.050

Terms of use:

Open Access

Anyone can freely access the full text of works made available as "Open Access". Works made available under a Creative Commons license can be used according to the terms and conditions of said license. Use of all other works requires consent of the right holder (author or publisher) if not exempted from copyright protection by the applicable law.

(Article begins on next page)



UNIVERSITÀ DEGLI STUDI DI TORINO

This is an author version of the contribution published on:
Questa è la versione dell'autore dell'opera:
[Bioorganic & Medicinal Chemistry 2015, 23, pp 4688–4698,
<http://dx.doi.org/10.1016/j.bmc.2015.05.050>]

The definitive version is available at:
La versione definitiva è disponibile alla URL:
[<http://www.sciencedirect.com/science/journal/09680896>]

NO-donor thiocarbocyanines as multifunctional agents for Alzheimer's disease

Konstantin Chegaev^a, Antonella Federico^a, Elisabetta Marini^a, Barbara Rolando^a, Roberta Fruttero^{a*}, Michela Morbin^b, Giacomina Rossi^b, Valeria Fugnanesi^b, Antonio Bastone^c, Mario Salmona^c, Nahuai B. Badiola^d, Laura Gasparini^d, Sara Cocco^e, Cristian Ripoli^e, Claudio Grassi^e, Alberto Gasco^a

^aDipartimento di Scienza e Tecnologia del Farmaco, Università degli Studi di Torino, via Pietro Giuria 9, 10125 Torino, Italy.

^bDivision of Neurology V and Neuropathology, Fondazione IRCCS Istituto Neurologico Carlo Besta, Milano, Italy.

^cDepartment of Molecular Biochemistry and Pharmacology, IRCCS-Istituto di Ricerche Farmacologiche "Mario Negri", Milano, Italy.

^dDepartment of Neuroscience and Brain Technologies, Istituto Italiano di Tecnologia, Genova, Italy

^eInstitute of Human Physiology, Università Cattolica, Roma, Italy

*Corresponding Author. E-mail: roberta.fruttero@unito.it. Phone: (+39) 0117607850, fax: (+39) 0116707286.

Keywords. Alzheimer disease, nitric oxide, β -amyloid, tau proteins, thiocarbocyanines, long term potentiation.

ABSTRACT

Some symmetrical and unsymmetrical thiocarbocyanines bearing NO-donor nitrooxy and furoxan moieties were synthesized and studied as candidate anti-Alzheimer's drugs. All products activated soluble guanylate cyclase (sGC) in a dose-dependent manner, depending on the presence in their structures of NO-donor groups. None displayed toxicity when tested at concentrations below 10 μ M on human brain microvascular endothelial cells (hCMEC/D3). Some products were capable of inhibiting amyloid β -protein ($A\beta$) aggregation, with a potency in the low μ M concentration range, and of inhibiting aggregation of human recombinant tau protein

in amyloid fibrils when incubated with the protein at 1 μM concentration. Nitrooxy derivative **21** and furoxan derivative **22** were selected to investigate synaptic plasticity. Both products, tested at 2 μM concentration, counteracted the inhibition of long-term potentiation (LTP) induced by $\text{A}\beta_{42}$ in hippocampal brain slices.

1. Introduction

Dementia, remains one of the biggest global public health challenges. The number of people living with dementia worldwide today is estimated at 44 million, set to almost double by 2030 and more than triple by 2050.¹ Dementia syndrome is linked to a large number of underlying brain disorders, among which Alzheimer's disease (AD) is the most common. AD is a multifactorial neurodegenerative disease that is characterized by memory loss, cognitive impairment, progressive dissolution of personality and loss of intellectual capacities. As a consequence, patients become unable to deal autonomously with everyday life. The clinical onset of AD is usually after the fifth decade of life, the disease progresses slowly (up to 15 years), and no disease-modifying treatments are currently available.² As a result, AD has a severe impact on patients' and their families' quality of life, and its economic burden is massive.

AD is neuropathologically defined by abundant proteinaceous deposits - i.e., extracellular amyloid plaques and intraneuronal neurofibrillary tangles – in limbic and cortical regions of the brain, accompanied by damage to brain capillaries,³ and loss of pyramidal, cholinergic, noradrenergic and serotonergic neurons.⁴ Extracellular amyloid plaques are principally composed of amyloid β -protein ($\text{A}\beta$), whereas intraneuronal neurofibrillary inclusions are formed of hyperphosphorylated tau protein that accumulates in selected areas of the brain.⁴⁻⁷ $\text{A}\beta$ derives from the enzymatic processing of amyloid precursor protein (APP) and self-assembles into insoluble amyloid fibrils and oligomeric soluble aggregates.⁸ Tau protein is principally expressed in the neurons, where it associates to and stabilizes microtubules (MTs). Under pathological conditions, tau protein dissociates from MTs and aggregates into insoluble filaments, which form neurofibrillary tangles and neuropil threads.⁹ A wealth of experimental data shows that the oxidative stress consequent on perturbation of the prooxidant/antioxidant balance, due to abnormal production of reactive oxygen (ROS) and nitrogen (RNS) species, and/or to depletion of the antioxidant defenses, is also an important early event in AD.¹⁰

There is now great interest, both in products capable of inhibiting the formation of A β plaques and tau inclusions, and in antioxidants, as potential drugs for the treatment of AD.^{7,10-13} Indeed, although substantial efforts have been made to develop disease-modifying treatments for AD based on inhibiting A β aggregation/formation, all known strategies face serious hurdles in clinical application, and there is an urgent need for safe and effective drugs.¹⁴ Among the novel candidates proposed for AD treatment, symmetrical thiocarbocyanine dyes have been considered, in particular as potent tau aggregation inhibitors.^{11,12} It is known that many thiocarbocyanine derivatives are π delocalized lipophilic cations that are able to passively cross cell membranes and accumulate within cells.¹²

Nitric oxide (NO) is an endogenous messenger essential for the functioning of the cardiovascular, nervous and immune systems.¹⁵ In the cardiovascular system, it displays vasodilator effects, reduces vascular smooth muscle cell (VSMCs) migration and proliferation, inhibits platelet adherence and aggregation, decreases leukocyte chemotaxis, and enhances VSMCs apoptosis.^{16,17} In the central nervous system, NO plays roles in regulating synaptic plasticity, neurosecretion, and the sleep-wake cycle.¹⁸ It can exert either neuroprotection or neurotoxicity, depending on its concentration. At high concentrations it is neurotoxic, in particular in the presence of oxidative stress, while at low physiological concentrations it confers protection through a number of mechanisms. These include: chain-breaking antioxidant activity and S-nitrosation of caspase and of the NR1 and NR2 subunits of the N-methyl-D-aspartate receptor.¹⁴ In addition, several reports provide experimental evidence that the NO/cGMP signaling pathway plays important roles in synaptic plasticity and acquisition of new learning and memory.^{19,20} Recent results show that endothelial derived NO (EDRF) modulates the expression and processing of APP.¹⁹ Neuroprotective activity, and an ability to restore LTP deficits, have been reported for a number of NO-donors belonging to the classes of nitrates and furoxans, which slowly release small amounts of NO.^{21,22} A number of NO chimeras have been proposed as therapeutic agents in Alzheimer's disease, including NO donor 4-methylthiazoles and NO donor tacrine/ferulic acid hybrids.^{23,24} As a continuation of research on NO-donor multitarget compounds,²⁵ some new NO chimeras obtained by grafting classical nitrate and furoxan NO-donors onto the thiocarbocyanine **1** are described (Chart 1). The synthesis,

antagonist activity against A β and tau protein aggregation, and capacity to activate the sGC of this new class of products are reported.

The ability of **21** and **22**, two of the most interesting products of the series, to exert protective effects against the A β_{42} -induced impairment of hippocampal LTP, which is the cellular correlate of memory,^{26,27} is also discussed.

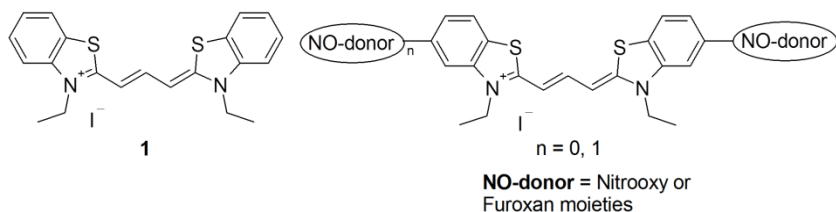
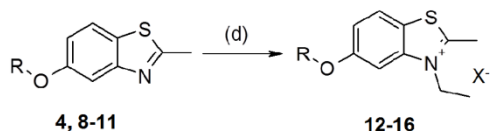
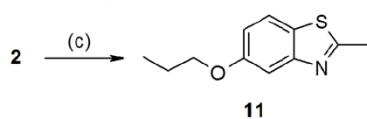
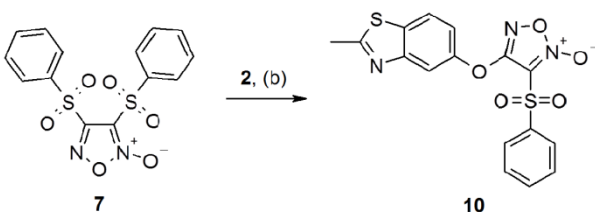
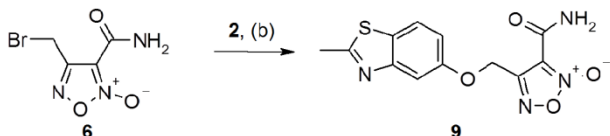
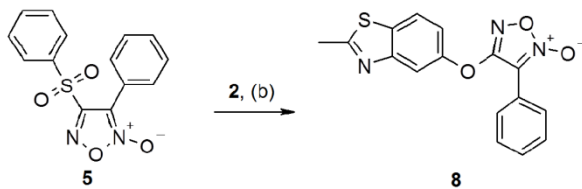
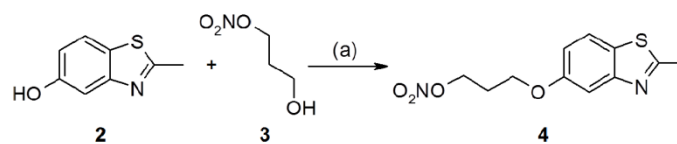


Chart 1. Thiocarbocyanine **1** and general structure of the related NO-donor chimeras

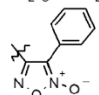
2. Results and discussion

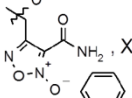
2.1. Chemistry

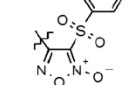
The intermediate quaternary salts used to prepare the symmetrical thiocarbocyanines were obtained through the synthetic pathway reported in Scheme 1. 2-Methyl-5-benzothiazolol (**2**) was coupled under Mitsunobu conditions with 3-hydroxypropyl nitrate (**3**) to afford the 3-nitrooxypropyloxy substituted 2-methylbenzothiazole (**4**). Furoxan derivatives **8-10** were synthesized starting from the furoxans **5-7** by reaction with **2** in dichloromethane (DCM) solution, in the presence of 1,8-diazabicyclo[5.4.0]undec-7-ene (DBU). It is known that under these conditions the phenylsulphonyl group at the 4-position of the furoxan **7** is selectively displaced.²⁸ The benzothiazole **11** was prepared from **2** and propyl bromide in the presence of potassium carbonate, using dimethylformamide (DMF) as solvent. The benzothiazoles **4**, **8-10** were transformed into the related quaternary salts **12-15** by treatment with ethyltrifluoromethanesulfonate in 1,2-dichloroethane solution. In the case of **11**, quaternarization was carried out in iodoethane to give the iodide **16**.



4, 12 R = (CH₂)₃ONO₂, X = CF₃SO₃⁻;

8, 13 R = , X = CF₃SO₃⁻;

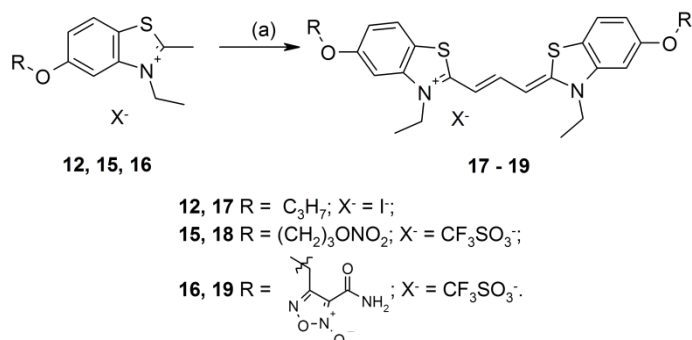
9, 14 R = , X = CF₃SO₃⁻;

10, 15 R = , X = CF₃SO₃⁻;

11, 16 R = C₃H₇, X = I⁻

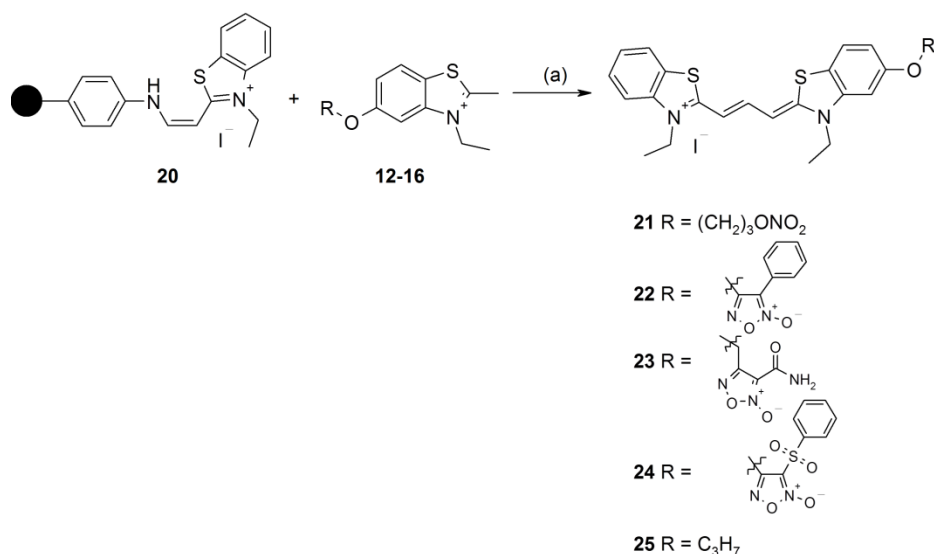
Scheme 1. Synthesis of compounds **4**, **8-16**. (a) DIAD, PPh₃, THF dry, 0°C to rt; (b) DBU, DCM; (c), *n*-C₃H₇Br, K₂CO₃, DMF dry; (d) C₂H₅OSO₂CF₃, ClCH₂CH₂Cl, for **12-15**; C₂H₅I, reflux for **16**.

The final symmetrically-substituted cyanines **17-19** were obtained by treating the respective quaternary salts in pyridine with triethylorthoformate at 110°C (Scheme 2).



Scheme 2. Synthesis of symmetrically-substituted cyanines **17-19**. (a) HC(OC₂H₅)₃, C₅H₅N, 110°C.

The monosubstituted cyanines **21-25** were prepared through a solid-phase method, as recently proposed for the synthesis of various cyanine dyes (Scheme 3).²⁹ A Merrefield resin was used to prepare the immobilized hemicyanine **20**, which was treated at room temperature with a sub-stoichiometric amount of the appropriate quaternary salts **12-16**, acetic anhydride (Ac₂O) and diisopropylethylamine (DIPEA) in pyridine. The resin was removed by filtration, and evaporation of the solvent gave the expected products **21-25**, which were purified by flash chromatography and crystallization.



Scheme 3. Synthesis of the monosubstituted cyanines **21-25**. (a) DIPEA, C₅H₅N, Ac₂O, rt.

2.2. Activation of sGC

NO modulates neuronal function through a number of mechanisms, among which the NO/sGC/cGMP signal transduction system is involved in synaptic plasticity, learning, and memory formation.³⁰ The capacity of the newly synthesized NO-donor cyanines to activate the production of cGMP in human brain micro-vascular endothelial cells (hCMEC/D3) was evaluated at 0.1-10 μ M concentrations, using the Cyclic GMP[³H] Assay System. This assay is based on competition between unlabeled cGMP and a fixed quantity of tritium-labeled compound to bind to an antiserum which has high specific affinity for cGMP. Sodium nitroprusside (SNP), a spontaneous NO-donor, was used as positive control for the test; cyanine **1** was used as negative control. Results are reported as ratios of pmol of cGMP produced to one million cells (Figure 1).

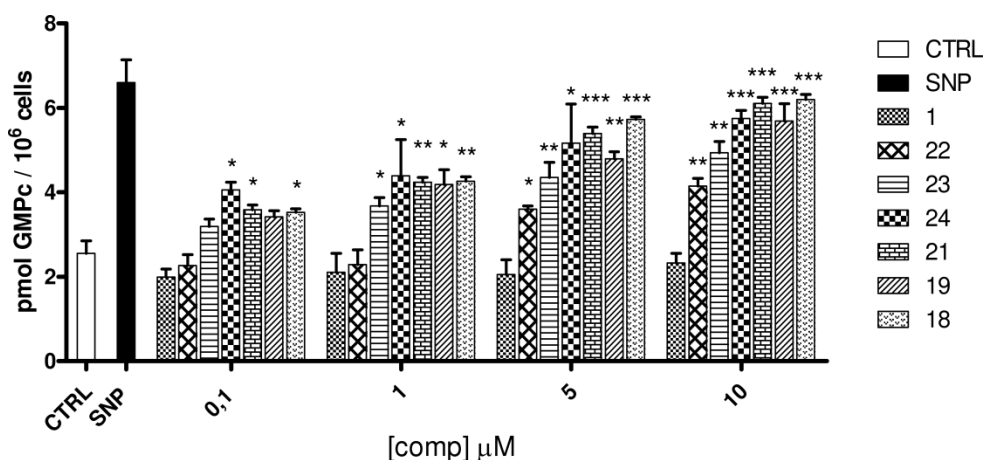


Figure 1. cGMP production in the hCMEC/D3 cells. All data presented are the mean \pm SEM * $p < 0.05$, ** $p < 0.01$ and *** $p < 0.0001$ vs CTRL. The results were analyzed by a one-way analysis of variance (ANOVA). A $p < 0.05$ was considered significant.

As expected, compound **1** did not influence the production of cGMP vs control. By contrast, all NO-donor cyanines were able to produce significant amounts of cGMP in a dose dependent manner. In the furoxan series the activity of furoxans **23** and **24** was higher than that of furoxan **22** and this is in keeping with reports that NO release from furoxan system is potentiated by the presence of an electron withdrawing substituent at the 3- position of the ring.³¹ In the nitrooxy series, both the monosubstituted and the disubstituted cyanines showed equal capacity for sGC activation. The same microvascular endothelial cells (hCMEC/D3) were used

to determine the cytotoxicity of the cyanine derivatives, using the lactate dehydrogenase (LDH) assay. No significant toxicity was detected up to 1 μM concentration for any of the compounds. Some products showed moderate toxicity at 10 μM concentration, and higher toxicity at 20 μM concentration (see supporting material).

2.3 Beta-Amyloid assay

A β aggregation is a complex process, and not yet fully understood. It is reported that the conformation adopted by A β peptides is of paramount importance.⁸ When the peptide adopts the random coil/ α -helical structure, aggregation occurs slowly, whereas the β -sheet conformation accelerates the process.³² The ability of the synthesized compounds to inhibit A β_{40} amyloid protein aggregation was evaluated using LeVine's classic spectrofluorimetric method, based on fluorescence emission (482 nm) of Thioflavin T (ThT).^{33,34} ThT fluorescence is enhanced upon binding to A β fibrils in proportion to the amount of fibrils in solution. The results are reported in Table 1, expressed as IC₅₀ or, for the less potent compounds, as % inhibition at the highest concentration tested (100 μM). Methylene blue (MB) was taken as a reference compound. It is known that some benzothiazole cyanine derivatives with specific structural properties, can bind aggregated amyloid and therefore interfere with ThT binding.³⁵ In this study compounds **21** and **22**, taken as representatives of the furoxan and nitrooxy families of hybrids, did not affect ThT binding to aggregated amyloid (see experimental part).

Table 1 shows that inhibition of aggregation is strongly influenced by the substitution pattern of the cyanine. All three symmetrically-disubstituted compounds (**17** – **19**) displayed only very low antiaggregatory activity, when tested at 100 μM concentration; attention was thus directed principally to the monosubstituted derivatives. The products are too few and the aggregation process too complex to determine clear structure-activity relationships, and only some disjointed considerations are possible. Product **21** and its des-NO analogue **25**, which bear linear lipophilic nitrooxypropyloxy and propyloxy chains respectively, display similar high potency, in the low μM concentration range in which **1** is active. In the derivatives belonging to the furoxan series, compound **23**, in which the furoxan ring bears the highly hydrophilic 3-carbamoyl moiety as substituent, is only a very weak antiaggregatory agent, conversely, the cyanine **22**, in which the furoxan ring is substituted with the lipophilic phenyl group, is the most

potent agent of the series. Insertion into this model of the bulky SO₂ bridge, between the hetero ring and the phenyl group, gives rise to compound **24**, having intermediate antiaggregatory potency. The most active products **1**, **21**, **22** and **25**, were also tested for their ability to inhibit aggregation of the more synaptotoxic A β ₄₂ amyloid protein. The results, in Table 1, generally parallel those obtained with the A β ₄₀ form, with the sole exception of **25**, which is about ten times more potent as an inhibitor of the A β ₄₂ form.

Table 1. Inhibition of A β ₄₀ and A β ₄₂ aggregation by NO-donor cyanines and by lead **1**.

Compd	A β ₄₀ aggregation inhibition	A β ₄₂ aggregation inhibition
	IC ₅₀ (μ M) (CL95%) [% of inhibition \pm SE] ^a	IC ₅₀ (μ M) (CL95%)
MB	4.5 (2.5-8.1); 2.3 ¹²	
1	3.1 (1.8-5.5)	3.3 (1.5-5.0)
17	N.A. ^b	
18	[26 \pm 9]	
19	[17 \pm 11]	
21	8.1 (5.5-12)	7.7 (1.8-14)
22	1.8 (1.4-2.3)	1.6 (0.07-3.2)
23	[26 \pm 4]	
24	21 (12-38)	
25	7.0 (5.5-9.0)	0.8 (0.47-1.1)

^a % of inhibition at the highest concentration tested (100 μ M).

^b N.A: not active at the highest concentration tested (100 μ M).

2.4. Tau protein aggregation assays

Tau protein is the main target of cyanine dyes. Fibril aggregation of tau is a complex multistep phenomenon, which begins with the formation of diffusible oligomeric structures that evolve into fibrils with a characteristic β -sheet motif. Recent studies indicate that cyanine dyes inhibit the formation of tau fibrils by disrupting tau oligomers.^{12,36} In order to explore the capacity of the new compounds to inhibit tau protein aggregation in fibrils, the lead **1** and NO donor cyanines **21**, **22**, **24**, which trigger good β -amyloid anti-aggregation activity, together with the product **18**, as an example of a symmetrically-substituted cyanine, were co-incubated with tau protein to examine the effects of these molecules on the fibrillogenic properties of the protein. Changes to the aggregation rate at different times, and the morphology of the aggregates, were evaluated by electron microscopy (EM); the amount of aggregates arranged in β -sheet secondary structure was evaluated with Congo Red (CR) histochemical dye. CR binds β -sheet-rich structures, and this interaction is revealed by the appearance of apple-green birefringence under polarized light. By contrast, red or yellow birefringence indicates the presence of β -sheet-free amorphous aggregates (Figure 2).³⁷

Wild-type (wt) human tau isoform 2N4R (441 aa) at 8 μ M final concentration was incubated for a short (48 h) or a long time (5 days). The staining properties and ultrastructure of aggregates generated by tau wt alone, by cyanine-NO donor hybrids **18**, **21**, **22** and **24** alone (1 μ M final concentration) or by co-incubation of tau wt and the above products were determined. At each time point, aliquots of peptide suspension were negatively stained with uranyl acetate and analysed by EM, or stained with Congo Red and examined under polarized light (Figure 2).

EM analysis showed that cyanine-NO donor hybrids **18**, **21**, **22** and **24** did not generate fibrils at any time points whereas tau wt readily aggregated into straight, unbranched fibrils, often twisted, mingled with amorphous materials, oligomers, and protofibrils, starting from 2 days' incubation (Figure 2A). Amyloid progressively increased up to 5 days, when the samples contained long, straight, unbranched 8-10 nm fibrils, many of them organized in a loose meshwork (Figure 2B). When tau protein was co-incubated with each of the selected compounds, both the formation rate and the number of aggregates formed were reduced. Oligomers and protofibrils predominated, and the few fibrils detectable - but only after 5 days incubation - were irregular and more varied in size than those formed by tau protein alone (Figure 2C, D, E, F).

Co-incubation with any of the selected compounds affected the fibrillogenic capability of tau protein. However, they differed in anti-fibrillogenic activity, compound **24** being the strongest inhibitor (data not shown) and compound **1** the weakest (Figure 2C, D, I, J), while hybrids **18**, **21**, **22** displayed intermediate inhibitory activity. In particular, compounds **21** and **22**, which possess marked, though different, A β -antiaggregation capability, also strongly impaired the fibrillogenesis of tau protein: after 2 days of incubation, the mixtures tau/compound **21** and tau/compound **22** contained only oligomers, amorphous materials, and occasional protofibrils, no amyloid-fibrils being present (Figure 2E). Even after 5 days of incubation, very few protofibrils and almost no amyloid fibrils were detectable (Figure 2F).

Congo Red staining confirmed that none of the compounds as such showed any positivity under polarized light, whereas the macromolecular assemblies of tau protein showed the staining and optical properties typical of in situ amyloid - i.e. birefringence under polarized light. These properties were already confirmed at day 2 (Figure 2G) and were more apparent after longer incubation times, as both the number and the size of aggregates increased (Figure 2H). Conversely, in samples containing the tau/cyanine mixtures, fewer and smaller birefringent aggregates were observed after 2 days (Figure 2I, K); although they increased with time, they did not reach the size and density of tau wt even after 5 days (Figure 2J, L). In particular, aggregates generated by tau/cyanine compounds **21** and **22** did not possess the staining properties of amyloid, only a few small apple-green spots being observed at longer incubation times (Figure 2L). The ability of the compounds to inhibit tau protein aggregation, evaluated in a semi-quantitative manner, followed the order **24**>**18**~**21**~**22**>**1** (see supplemental material).

Intriguingly, the anti-aggregation activities of these compounds versus A β and versus tau were not equivalent: the thioflavin test for A β aggregation, and morphological and CR semi-quantification for tau protein aggregation, showed that furoxan **24**, the compound producing the strongest inhibition of tau protein aggregation, displayed only moderate A β -antiaggregation potency, and the symmetrical dinitrooxy propyloxy substituted cyanine **18**, endowed with poor A β -antiaggregation capacity, interacted with tau protein greatly reducing its fibrillogenic capability. Conversely, the mononitrooxy analogue **21** and furoxan **22**, which significantly impair fibrillar tau-aggregation, are also potent inhibitors of A β fibrillar aggregation. These findings suggest that the structural features underlying A β and tau antiaggregation in this class of

products are not necessarily the same. As discussed above for A β aggregation, it is not possible to find out a clear structure – activity relationship for the anti-amyloidogenic ability of the products since amyloid formation is a complex, multistep process in which a given molecule may act more or less potently at different aggregation steps.

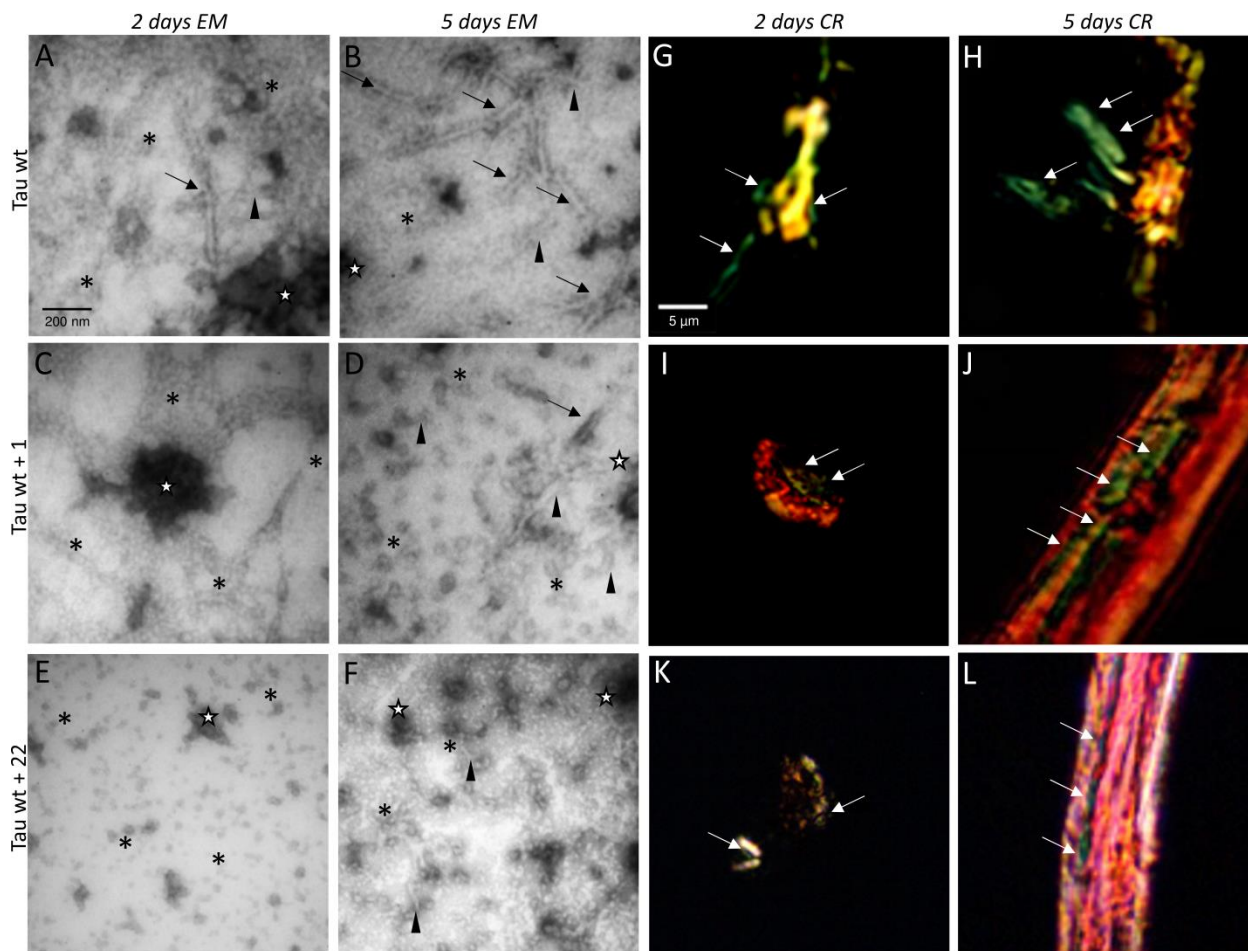


Figure 2. Electron microscopy (A-F) and CR birefringence (G-L) of aggregates generated by wt tau protein (8 μ M) in the absence and presence of cyanines (1 μ M). Tau alone after 2 (A, G) and 5 (B, H) days of incubation; tau + **1** after 2 (C, I) and 5 (D, J) days; tau + **22** after 2 (E, K) and 5 (F, L) days. Images A-F are at the same magnification; scale-bar = 200 nm. Stars = amorphous material; asterisks = oligomers; arrowheads = protofibrils; arrows = fibrils. Images G-L are at the same magnification; scale-bar = 5 μ m. White arrows = Apple-green birefringence indicative of β -sheet-rich structures.

2.5. Study of long-term synaptic potentiation

Many studies have shown that hippocampal brain slices of rodents exposed to nanomolar concentrations of human A β ₄₂ display impaired LTP.³⁸⁻⁴² In the present study it was found that, following high frequency stimulation (HFS) field excitatory postsynaptic potential (fEPSP) amplitudes increased by +98.0 \pm 8.5% (n=33) over baseline in control conditions, and by +24.0 \pm 8.0% (n=19) after exposure to 200 nM A β ₄₂ (P <0.01, Figure 3). LTP inhibition was significantly lower following co-application of 200 nM A β ₄₂ plus 2 μ M nitrate hybrid **21**: under this experimental condition, mean fEPSP amplitude was +69.3 \pm 13.0% baseline (n=9, P <0.01, Figure 3). Brain slice treatment with 2 μ M compound **22** provided a stronger protective effect against A β ₄₂-induced LTP inhibition, raising the fEPSP amplitude to +90.8 \pm 7.9% baseline (n=10, P <0.01 versus A β ₄₂ alone; not significant versus controls, Figure 3), whereas exposure of slices to compound **1** plus A β ₄₂ produced an increase in the fEPSPs amplitude similar to that observed with A β ₄₂ alone (+34.7 \pm 7.9%, n=7). In control experiments, application of **21** or **22** in the absence of A β ₄₂ slightly but not significantly increased LTP versus vehicle (+110.4 \pm 23.2%, n=13, and +111.9 \pm 11.9%, n=7, respectively), whereas LTP following application of **1** alone was slightly but not significantly lower than vehicle (+82.4 \pm 12.4%, n=5).

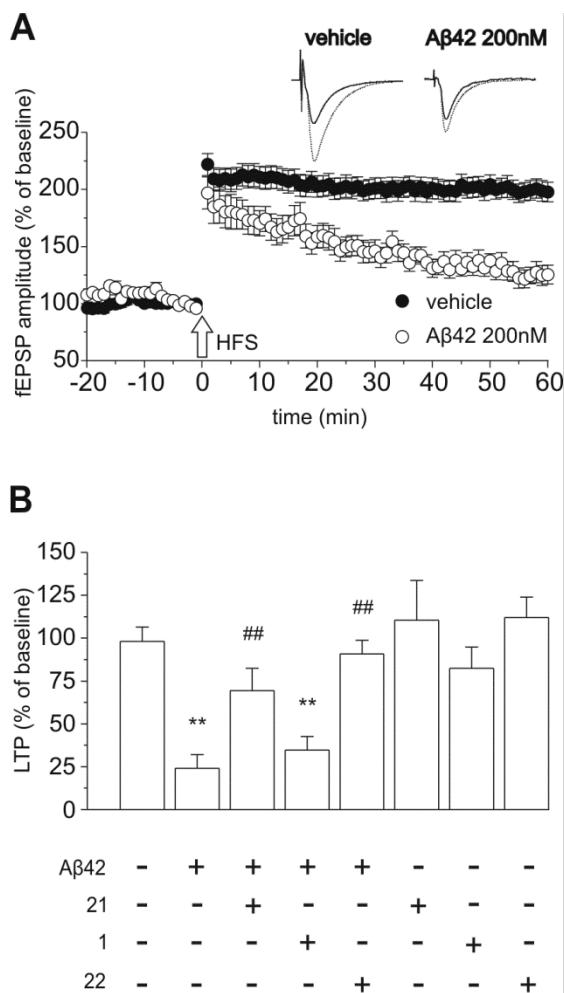


Figure 3. Effects of compounds **21**, **1** and **22** on A β -induced inhibition of LTP in hippocampal brain slices. **A.** Time course of fEPSP amplitudes before and after HFS (indicated by arrow) in control slices (dots) and following 20 min treatment with 200 nM A β ₄₂ (circles). Insets show representative fEPSPs at baseline (solid line) and during the last 5 min of LTP recording (dotted line). Results are expressed as percentages of baseline fEPSP amplitude (=100%). **B.** LTP amplitudes measured during the last 5 min of recordings (from 55 to 60 min post HFS) under the conditions described below the bar graph. ** P<0.01 vs. controls; ## P<0.01 vs. 200 nM A β ₄₂. All data presented are mean \pm SEM. Statistical analyses (Student's unpaired t tests) were performed with SYSTAT 10.2 software (Statcom). A p < 0.05 was considered significant.

As was said above, numerous studies report that rodent brain slices exposed to nanomolar concentrations of human A β ₄₂ show reduced hippocampal LTP⁴³, which is the cellular correlate

of memory.^{26,27} The finding that products **21** and **22** provide significant relief from the A β ₄₂-induced toxic effects on LTP, demonstrates their ability to ameliorate AD-associated synaptic dysfunction. Of note, synaptic function impairment correlates with early stages of AD prior to neuronal loss.⁴⁴ Furthermore, studies on transgenic AD mice suggest that early pharmacological interventions might reverse the AD phenotype.⁴⁵ Thus, products **21** and **22** which are able to restore A β ₄₂-induced inhibition of LTP could have a therapeutic effect in treating AD-associated impairment of synaptic plasticity.

3. Conclusions

In search of new drugs potentially useful in the treatment of AD, a strategy focused on both A β and tau aggregation inhibition was followed, designing a series of thiocarbocyanines joined to NO-donor moieties. The goal was to obtain multitarget drugs endowed simultaneously with the beneficial effects of NO on synaptic plasticity, and with the β -amyloid/tau protein antiaggregatory properties of cyanine derivatives. All compounds were able to activate sGC and displayed low toxicity on human brain microvascular endothelial cells in the lactate dehydrogenase test. Some compounds were capable of inhibiting aggregation both of β -amyloid and of tau proteins. Products **21**, containing a NO-donor nitrooxy function, and **22**, containing the NO-donor 3-phenyl furoxan system, selected for LTP studies in hippocampal brain slices, protected synaptic plasticity from A β ₄₂-induced damage. The results of this study show that insertion of NO-donor nitrooxy and furoxan moieties onto the thiocarbocyanine scaffold can provide multitarget products with therapeutic potential in Alzheimer's disease worthy of additional *in vivo* studies.

4. Experimental

4.1. Chemistry

¹H and ¹³C NMR spectra were recorded on a BrukerAvance 300, at 300 and 75 MHz, respectively, using SiMe₄ as internal standard. The following abbreviations indicate peak multiplicity: s = singlet; d = doublet; t = triplet; q = quartet; qi = quintet, m = multiplet, bs = broad singlet. Other abbreviations: Btz = benzothiazole. Low-resolution mass spectra were recorded with a ThermoFinnigan LTQ (Ion Trap). ESI spectra were recorded on Micromass

Quattro API micro (Waters Corporation, Milford, MA, USA) mass spectrometer. Data were processed using a MassLynxSystem (Waters). Melting points were determined with a capillary apparatus (Büchi 540) in open capillary. Flash column chromatography was performed on silica gel (Merck Kieselgel 60, 230–400 mesh ASTM). The progress of the reactions was followed by thin-layer chromatography (TLC) on 5 × 20 cm plates Merck Kieselgel 60 F₂₅₄, with a layer thickness of 0.20 mm. HPLC analyses were performed with a HP 1100 HPLC system (Agilent Technologies, Palo Alto, CA, USA) equipped with a quaternary pump (model G1311A), a membrane degasser (G1379A) and a diode-array detector (DAD) (model G1315B) integrated into the HP1100 system. Data analysis was done using a HP ChemStation system (Agilent Technologies). The analytical column was a Lichrospher C18 (4.6 × 250 mm, 5 μm) Merck, the eluates were analyzed at λ 226 nm, 254 nm and 542 nm (vs 700 nm). Anhydrous sodium sulfate (Na₂SO₄) was used as drying agent for the organic phases. Organic solvents were removed under reduced pressure at 30°C. Synthetic-purity solvents ethyl acetate (EtOAc), acetone, hexane, dichloromethane (DCM), acetonitrile (CH₃CN), methanol (MeOH), diethyl ether (Et₂O), dimethylformamide (DMF) and 40–60 petroleum ether (PE) were used without further purification. Dry tetrahydrofuran (THF), was distilled immediately before use from Na and benzophenone under positive N₂ pressure. Dry DCM was distilled from P₂O₅ and kept on 4Å molecular sieves. Dry DMF was obtained through storage on 4Å molecular sieves. Dry pyridine was distilled from KOH and kept on 4Å molecular sieves under N₂. Commercial starting materials were purchased from Sigma-Aldrich, Alfa Aesar, and TCI Europe. Elemental analyses (C, H, N) of the target compounds were performed by Section de Pharmacie, Service de Microanalyse (Geneva). Compounds **1**,⁴⁶ **3**,⁴⁷ **5**,⁴⁸ **6**⁴⁹ and **7**⁵⁰ were synthesized following methods described in the literature.

3-[(2-Methyl-1,3-benzothiazol-6-yl)oxy]propyl nitrate (4). To a stirred solution of PPh₃ (2.61 g, 9.96 mmol) in dry THF (15 mL) under positive nitrogen pressure, diisopropylazodicarboxylate (DIAD) (2 mL, 9.96 mmol) was added at 0°C. Stirring was continued for 15 min at room temperature, then **2** (1.14 g, 8.3 mmol) was added, followed after 20 minutes by **3** (1.00 g, 6.05 mmol). The mixture was stirred for 24 hours at rt. The reaction mixture was concentrated and the resulting brown oil was purified by flash chromatography (eluent PE/EtOAc 70/30 v/v). The resulting solid was crystallized from diisopropylether to give

4 as a white solid; yield 65%. M.p. 71.5-72.5°C (*i*-Pr₂O). ¹H-NMR (CDCl₃) δ (ppm): 2.24 (m, 2H, CH₂CH₂CH₂), 2.81 (s, 3H, CH₃), 4.12 (t, 2H, OCH₂CH₂CH₂ONO₂), 4.69 (t, 2H, CH₂ONO₂), 6.98 (dd, 1H), 7.42 (d, 1H), 7.66 (d, 1H) (Btz); ¹³C-NMR (CDCl₃) δ (ppm): 20.1, 26.9, 63.8, 69.9, 105.8, 114.7, 121.7, 127.8, 154.4, 157.5, 168.4. MS EI *m/z* 268 (M)⁺.

General procedure for the synthesis of furoxan derivatives 8-10. To a solution of **2** (300 mg, 1.81 mmol) in DCM (25 mL), the appropriate furoxan (2.17 mmol) and DBU (324 μL, 2.17 mmol) were added. The mixture was stirred at room temperature and monitored by TLC. Once the reaction had terminated, the remainder was washed with water (2×10 mL), NaOH 1M (2×10 mL), HCl 1M (2×10 mL), and brine, dried, and evaporated. Crude products thus obtained were purified as described.

2-Methyl-5-[(3-phenylfuroxan-4-yl)oxy]-1,3-benzothiazole (8). The reaction was stirred at room temperature overnight, the title compound was crystallized from ethanol; white powder; yield 53%. M.p. 112.0-113.0°C (EtOH). ¹H-NMR (CDCl₃) δ (ppm): 2.86 (s, 3H, CH₃), 7.39 (dd, 2H), 7.51 – 7.58 (m, 3H), 7.87 (d, 1H), 7.94 (d, 1H), 8.23 (d, 2H) (Btz, C₆H₅); ¹³C-NMR (CDCl₃) δ (ppm): 20.3, 107.8, 113.9, 117.3, 122.0, 122.3, 126.4, 129.0, 130.7, 133.6, 151.1, 154.1, 162.2, 169.8. MS EI *m/z* 325 (M)⁺.

4-[(2-Methyl-1,3-benzothiazol-5-yl)oxy]methyl-furoxan-3-carboxamide (9). The reaction was stirred at room temperature overnight, the title compound was crystallized from isopropanol; white powder; yield 61.8%. M.p. 185.0-190.0°C dec. (*i*-PrOH). ¹H-NMR (DMSO-*d*₆) δ (ppm): 2.77 (s, 3H, CH₃), 5.50 (s, 2H, OCH₂), 7.12 (dd, 1H), 7.60 (d, 1H), 7.92 (d, 1H) (Btz), 7.85 (bs 1H), 8.50 (bs, 1H, NH₂); ¹³C-NMR (DMSO-*d*₆) δ (ppm): 19.8, 61.6, 106.6, 110.5, 114.5, 122.4, 127.8, 154.1, 155.2, 155.7, 156.7, 168.5. MS CI *m/z* 307 (M+1)⁺.

2-Methyl-5-[[3-phenylsulfonylfuroxan-4-yl]oxy]-1,3-benzothiazole (10). The reaction was stirred at room temperature overnight, the title compound was crystallized from isopropanol; white powder; yield 50.0%. M.p. 137.5-138.0°C (*i*-PrOH). ¹H-NMR (CDCl₃) δ (ppm): 2.86 (s, 3H CH₃), 7.34 (dd, 1H), 7.65 (t, 2H), 7.77 – 7.88 (m, 3H), 8.12 (d, 2H) (C₆H₅ + Btz); ¹³C-NMR (CDCl₃) δ (ppm): 20.3, 110.7, 113.7, 117.2, 122.4, 128.6, 129.8, 134.0, 135.9, 137.9, 151.0, 154.1, 158.7, 170.0. MS EI *m/z* 389 (M)⁺.

2-Methyl-5-propoxy-1,3-benzothiazole (11). To a solution of **2** (500 mg, 3.02 mmol) in DMF (15 mL) K_2CO_3 (209 mg, 1.51 mmol) and 1-bromopropane (0.30 mL, 3.32 mmol) were added. The mixture was stirred at 60°C overnight. The reaction mixture was diluted with H_2O (30 mL) and extracted with AcOEt (40 mL), the organic phase was washed with NaOH 1M (2×10 mL), HCl 1M (2×10 mL), brine, dried and evaporated to give a yellow solid. The product was purified by flash chromatography (eluent DCM/MeOH 99/1 v/v); white powder; yield 64%. 1H -NMR ($CDCl_3$) δ (ppm) 1.06 (t, 3H, CH_2CH_3), 1.85(m, 2H, $OCH_2CH_2CH_3$), 2.80 (s, 3H, CH_3Btz), 3.98 (t, 2H, OCH_2), 6.99 (dd, 1H), 7.44 (d, 1H), 7.63 (d, 1H) (Btz); ^{13}C -NMR ($CDCl_3$) δ (ppm): 10.6, 20.2, 22.5, 69.9, 105.9, 115.1, 121.5, 127.1, 154.6, 158.3, 168.1. MS EI m/z 207 (M)⁺.

General procedure for the synthesis of quaternary salts 12-16. To a solution of benzothiazole derivative (1.12 mmol) in 1,2-dichloroethane (10 mL) ethyltriflate (289 μ L, 2.24 mmol) was added and the reaction was stirred under positive N_2 pressure for the time indicated. Products were purified as described.

3-Ethyl-2-methyl-5-[3-(nitrooxy)propoxy]-1,3-benzothiazol-3-ium trifluoromethanesulfonate (12). The reaction was stirred at room temperature overnight, the title compound was purified by flash chromatography (eluent 95/5 DCM/MeOH v/v); white solid; yield 56.0%. 1H -NMR ($DMSO-d_6$) δ (ppm): 1.45 (t, 3H, CH_3CH_2N), 2.24 (qi, 2H $OCH_2CH_2CH_2$), 3.18 (s, 3H, CH_3Btz), 4.30 (t, 2H, OCH_2), 4.75 (m, 4H, $CH_2ONO_2 + CH_2N$), 7.43 (dd, 1H), 7.82 (d, 1H), 8.30 (d, 1H) (Btz); ^{13}C -NMR ($DMSO-d_6$) δ (ppm): 13.1, 16.6, 26.1, 44.5, 65.4, 70.9, 100.4, 118.1, 118.5, 121.1, 125.4, 142.0, 159.7, 176.8. MS ESI⁺ m/z 297.2 (M)⁺.

3-Ethyl-2-methyl-5-[(3-phenylfuroxan-4-yl)oxy]-1,3-benzothiazol-3-ium trifluoromethanesulfonate (13). The reaction was stirred at room temperature overnight, the title compound was purified by flash chromatography (eluent 95/5 DCM/MeOH v/v); white powder; yield 60.0%. 1H -NMR ($DMSO-d_6$) δ (ppm): 1.44 (t, 3H, CH_3CH_2N), 3.25 (s, 3H, CH_3Btz), 4.73 (m, 2H, CH_2N), 7.62 – 7.69 (m, 3H), 8.03 (dd, 1H), 8.11 (dd, 2H), 8.60 (d, 1H), 8.66 (d, 1H); ^{13}C -NMR ($DMSO-d_6$) δ (ppm): 13.1, 17.0, 45.1, 108.4, 108.7, 121.0, 121.4, 126.4, 126.7, 127.0, 129.2, 131.1, 141.5, 153.3, 162.0, 179.2. MS ESI⁺ m/z 354.2 (M)⁺.

5-[(3-Carbamoylfuroxan-4-yl)methoxy]-3-ethyl-2-methyl-1,3-benzothiazol-3-ium trifluoromethanesulfonate (14). The reaction was stirred at 50°C overnight, the title compound was purified by crystallization from *i*-PrOH; white solid; yield 80.0%. M.p. 178.5-179.5°C (*i*-PrOH). ¹H-NMR (DMSO-*d*6) δ (ppm): 1.43 (t, 3H, CH₃CH₂N), 3.17 (s, 3H, CH₃Btz), 4.72 (q, 2H, CH₂N), 5.67 (s, 2H, OCH₂), 7.52 (dd, 1H), 7.98 (s, 1H), 8.32 (d, 1H) (Btz), 7.88 (bs, 1H), 8.54 (bs, 1H) (NH₂); ¹³C-NMR (DMSO-*d*6) δ (ppm): 13.1, 16.6, 44.6, 62.0, 101.3, 110.6, 117.6, 121.9, 125.5, 141.9, 154.9, 155.7, 158.9, 177.3. MS ESI⁺ *m/z* 335.2 (M⁺).

3-Ethyl-2-methyl-5-[[3-phenylsulfonylfuroxan-4-yl]oxy]-1,3-benzothiazol-3-ium trifluoromethanesulfonate (15). The reaction was stirred at room temperature overnight, the title compound was purified by crystallization from *i*-PrOH; white powder; yield 80.6%. M.p. 189.0-190.5°C (*i*-PrOH). ¹H-NMR (DMSO-*d*6) δ (ppm): 1.43 (t, 3H, CH₃CH₂N), 3.23 (s, 3H, CH₃Btz), 4.69 (q, 2H, CH₂N), 7.76 (t, 2H), 7.93 (m, 2H), 8.01 (d, 2H), 8.48 (d, 1H), 8.54 (d, 1H), (C₆H₅+Btz); ¹³C-NMR (DMSO-*d*6) δ (ppm): 13.1, 16.8, 45.0, 107.6, 111.6, 120.3, 126.5, 127.0, 128.6, 130.0, 136.4, 136.6, 141.5, 153.8, 157.9, 179.4. MS ESI⁺ *m/z* 418.0 (M⁺).

3-Ethyl-2-methyl-5-propoxy-1,3-benzothiazol-3-ium iodide (16). A solution of **11** (900 mg, 4.35 mmol) in iodoethane (15 mL) was heated under reflux for one week. The precipitate obtained was filtered and washed with Et₂O. The crude **16** was used without further purification; pale green powder; yield 77%. ¹H-NMR (DMSO-*d*6) δ (ppm): 1.02 (t, 3H, CH₃CH₂CH₂O), 1.44 (t, 3H, CH₃CH₂N), 1.80 (m, 2H, CH₂CH₂O), 3.19 (s, 3H, CH₃Btz), 4.15 (t, 2H, CH₂O), 4.76 (q, 2H, CH₂N), 7.40 (d, 1H), 7.79 (s, 1H), 8.31 (d, 1H) (Btz); ¹³C-NMR (DMSO-*d*6) δ (ppm): 10.4, 13.2, 16.9, 21.8, 44.6, 70.3, 100.3, 118.0, 120.6, 125.3, 142.0, 160.0, 176.5. MS ESI⁺ *m/z* 236.2 (M⁺).

General procedure for the synthesis of 5,5'-disubstituted cyanines 17-19. Quaternary salts (1.34 mmol) and ethylorthoformate (4.02 mmol, 440 μL) were refluxed in 4 mL of pyridine. The reaction mixture was cooled to rt and Et₂O (10 mL) was added. The precipitate formed was filtered, washed with Et₂O and purified by flash chromatography (gradient from DCM to DCM/MeOH 98/2 v/v). The resulting compounds were further purified by crystallization from methanol to give a dark purple solid.

3-Ethyl-5-propyloxy-2-[3-(5-propyloxy-3-ethyl-1,3-benzothiazol-2(3*H*)-ylidene)prop-1-en-1-yl]-1,3-benzothiazol-3-ium iodide (17). Reaction time 2.5 h; yield 54.6%. M.p. 281-283°C dec. (MeOH). ¹H-NMR (DMSO-*d*₆) δ (ppm): 1.01 (t, 6H, 2CH₃CH₂CH₂O), 1.32 (t, 6H, 2CH₃CH₂N), 1.77 (m, 4H, 2CH₂CH₂O), 4.03 (t, 4H, CH₂O), 4.36 (q, 4H, 2CH₂N), 6.55 (d, 2H, CH=CH-CH, ³J_{HH}=12.8 Hz), 7.01 (d, 2H), 7.30 (s, 2H), 7.83 (d, 2H) (2Btz), 7.68 (t, 1H, CH=CH-CH, ³J_{HH}=12.8 Hz); ¹³C-NMR (DMSO-*d*₆) δ (ppm): 10.30, 12.5, 21.9, 41.3, 69.8, 98.5, 99.1, 112.9, 116.0, 123.5, 142.0, 145.4, 159.4, 164.8. PHPLC = 100% (mobile phase: CH₃CN/0.1% CF₃COOH in H₂O 80/20 v/v, *t*_R = 15.57 min). MS ESI⁺*m/z* 481.1 (M⁺). Anal. (C,H,N).

3-Ethyl-5-[3-nitrooxypropyloxy]-2-[3-(5-[3-nitrooxypropyloxy]-3-ethyl-1,3-benzothiazol-2(3*H*)-ylidene)prop-1-en-1-yl]-1,3-benzothiazol-3-ium trifluoromethanesulfonate (18). Reaction time 1 h; yield 21.2%. M.p. 186-188°C dec. (MeOH). ¹H-NMR (DMF-*d*₇) δ (ppm): 1.44 (t, 6H, 2CH₃CH₂N), 2.30 (m, 4H, 2OCH₂CH₂), 4.29 (t, 4H, 2OCH₂), 4.49 (m, 4H, 2CH₂N), 4.82 (t, 4H, 2CH₂ONO₂), 6.67 (d, 2H, CH=CH-CH, ³J_{HH}=12.4Hz), 7.08 (d, 2H), 7.46 (s, 2H), 7.82 – 7.93 (m, 3H) (2Btz + CH=CH-CH); ¹³C-NMR (DMF-*d*₇) δ (ppm): 12.6, 26.9, 42.0, 65.5, 71.3, 99.2, 99.4, 113.8, 117.3, 124.0, 142.9, 146.2, 160.0, 165.8. PHPLC = 100% (mobile phase: CH₃CN/0.1% CF₃COOH in H₂O 55/45 v/v, *t*_R = 24.87 min). MS ESI⁺*m/z* 603.1 (M⁺). Anal. (C,H,N).

5-[(3-Carbamoylfuroxan-4-yl)methoxy]-2-[3-(5-[3-(carbamoylfuroxan-4-yl)methoxy]-3-ethyl-1,3-benzothiazol-2(3*H*)-ylidene)prop-1-en-1-yl]-3-ethyl-1,3-benzothiazol-3-ium trifluoromethanesulfonate (19). Reaction time 1.5 h; yield 64.9%. M.p. 195°C change crystal shape, 220-225°C dec. (MeOH). ¹H-NMR (DMSO-*d*₆) δ (ppm): 1.30 (t, 6H, 2CH₃CH₂N), 4.30 (m, 4H, 2CH₂N), 5.51 (s, 4H, 2OCH₂), 6.52 (d, 2H, CH=CH-CH, ³J_{HH}=12.6Hz), 7.06 (d, 2H), 7.41 (s, 2H) (2Btz), 7.64 (t, 1H, CH=CH-CH, ³J_{HH}=12.6Hz), 7.80 – 7.87 (m, 4H, Btz + 2NH₂), 8.53 (bs, 2H, 2NH₂); ¹³C-NMR (DMSO-*d*₆) δ (ppm): 12.6, 41.5, 61.8, 98.9, 99.8, 110.5, 113.1, 117.4, 123.7, 142.0, 155.0, 155.8, 158.3, 165.0. PHPLC = 98% (mobile phase: CH₃CN/0.1% CF₃COOH in H₂O 55/45 v/v, *t*_R = 5.85 min). MS ESI⁺ *m/z* 678.9 (M⁺). Anal. (C,H,N).

General procedure for the solid-state synthesis of cyanine dyes 21-25. To a suspension of solid phase-bound hemicyanine (2.47 g, 2.27 mmol) in pyridine (35 mL) an appropriate quaternary salt (0.35 mmol), Ac₂O (1.75 mL), and DIPEA (3.5 mL) were added and the mixture was stirred at room temperature. The resin was removed by filtration and extensively washed with DCM. The solvent was evaporated and the resulting violet solid was washed with Et₂O and then purified by flash chromatography (gradient from DCM to DCM/MeOH 98/2 v/v). The compounds obtained were crystallized from methanol to give the title compounds as a dark purple powders.

3-Ethyl-2-[(3-{3-ethyl-5-[3-(nitrooxy)propoxy]-1,3-benzothiazol-2(3H)-ylidene}prop-1-en-1-yl)-1,3-benzothiazol-3-ium iodide (21). Reaction time 1 h; yield 21%. M.p. 223-225°C dec. (MeOH). ¹H-NMR (DMF-*d*7) δ (ppm): 1.47 (m, 6H, CH₃CH₂N), 2.31 (qi, 2H, OCH₂CH₂CH₂ONO₂), 4.33 (t, 2H, OCH₂), 4.54 (m, 4H, CH₂N), 4.83 (t, 2H, CH₂ONO₂), 6.77 (m, 2H, CH=CH-CH), 7.13 (d, 1H), 7.45 – 7.52 (m, 2H), 7.63 (t, 1H), 7.85 (d, 1H), 7.93 – 8.09 (m, 3H) (Btz, CH=CH-CH); ¹³C-NMR (DMF-*d*7) δ (ppm): 12.5, 12.6, 26.9, 42.0, 42.2, 65.5, 71.3, 98.9, 99.6, 113.6, 114.1, 117.4, 123.4, 124.1, 125.5, 125.9, 128.5, 141.6, 142.9, 146.9, 160.0, 164.7, 166.3. PHPLC = 98% (mobile phase: CH₃CN/0.1% CF₃COOH in H₂O 55/45 v/v, *t*_R = 9.70 min). MS ESI⁺ *m/z* 484.0 (M⁺). Anal. (C,H,N).

3-Ethyl-2-[(3-{3-ethyl-5-[(3-phenylfuroxan-4-yl)oxy]-1,3-benzothiazol-2(3H)-ylidene}prop-1-en-1-yl)-1,3-benzothiazol-3-ium iodide (22). Reaction time 1 h; yield 22%. M.p. 250-255°C dec. (MeOH). ¹H-NMR (DMF-*d*7) δ (ppm): 1.42 – 1.50 (m, 6H, CH₃CH₂N), 4.48 – 4.62 (m, 2H, CH₂N), 6.78– 6.92 (m, 2H), (CH=CH-CH), 7.52 (t, 1H), 7.64-7.73 (m, 6H), 7.92 (d, 1H), 8.12 – 8.22 (m, 5H) CH=CH-CH, C₆H₅, Btz); ¹³C-NMR (DMF-*d*7) δ (ppm): 12.4, 12.7, 42.3, 42.4, 99.1, 100.4, 106.2, 108.7, 114.1, 117.8, 122.3, 123.6, 123.7, 124.6, 126.0, 127.0, 128.7, 129.5, 131.4, 141.5, 142.9, 147.5, 153.7, 165.0, 166.0. PHPLC = 98% (mobile phase: CH₃CN/0.1% CF₃COOH in H₂O 55/45 v/v, *t*_R = 12.32 min). MS ESI⁺ *m/z* 541.0 (M⁺). Anal. (C,H,N).

3-Ethyl-2-[(3-{3-ethyl-5-[(3-carbamoylfuroxan-4-yl)methoxy]-1,3-benzothiazol-2(3H)-ylidene}prop-1-en-1-yl)-1,3-benzothiazol-3-ium iodide (23). Reaction time 2h; yield 20%. M.p. 185-188°C dec. (MeOH). ¹H-NMR (DMF-*d*7) δ (ppm): 1.40 – 1.48 (m, 6H,

$\text{CH}_3\text{CH}_2\text{N}$), 4.44 – 4.58 (m, 4H, CH_2N), 5.69 (s, 2H, OCH_2), 6.74 – 6.86 (m, 2H, $\text{CH}=\text{CH}-\text{CH}$), 7.21 (d, 1H), 7.62 (t, 1H), 7.59 – 7.66 (m, 2H), 7.83 – 8.08 (m, 5H), 8.61 (bs, 1H) (Btz, $\text{CH}=\text{CH}-\text{CH}$, NH_2); ^{13}C -NMR (DMF-*d*7) δ (ppm): 12.6, 12.6, 42.1, 42.2, 62.5, 99.1, 99.6, 100.2, 111.2, 113.6, 114.0, 118.3, 123.4, 124.2, 125.5, 125.9, 128.5, 141.5, 142.9, 146.9, 155.8, 156.3, 159.2, 164.8, 166.1. PHPLC = 98% (mobile phase: $\text{CH}_3\text{CN}/0.1\% \text{CF}_3\text{COOH}$ in H_2O 55/45 v/v, t_R = 4.39 min). MS ESI⁺ m/z 522.0 (M^+). Anal. (C,H,N).

3-Ethyl-2-[(3-{3-ethyl-5-[(3-phenylsulfonylfuroxan-4-yl)oxy]-1,3-benzothiazol-2(3H)-ylidene)prop-1-en-1-yl]-1,3-benzothiazol-3-ium iodide (24). Reaction time 1.5 h; yield 20%. M.p. 180-182°C dec. (MeOH). ^1H -NMR (DMSO-*d*6) δ (ppm): 1.24 – 1.39 (m, 6H, $\text{CH}_3\text{CH}_2\text{N}$), 4.25 – 4.30 (m, 2H, $\text{CH}_3\text{CH}_2\text{N}$), 4.40 – 4.46 (m, 2H, $\text{CH}_3\text{CH}_2\text{N}$), 6.64 (d, 1H, $^3J_{\text{HH}} = 12.4\text{Hz}$), 6.75 (d, 1H, $^3J_{\text{HH}} = 12.8\text{Hz}$) ($\text{CH}=\text{CH}-\text{CH}$), 7.40 – 7.56 (m, 2H), 7.59 (t, 1H), 7.74 – 7.87 (m, 5H), 7.92 – 7.97 (m, 1H), 8.02 – 8.09 (m, 4H) (C_6H_5 , Btz, $\text{CH}=\text{CH}-\text{CH}$); ^{13}C -NMR(DMSO-*d*6) δ (ppm): 12.4, 12.7, 41.5, 41.7, 98.3, 99.8, 104.6, 111.4, 113.6, 116.2, 122.7, 123.1, 124.2, 125.3, 125.4, 128.1, 128.5, 130.0, 136.3, 136.6, 140.7, 142.0, 146.6, 152.9, 158.2, 164.3, 164.9. PHPLC = 98% (mobile phase: $\text{CH}_3\text{CN}/0.1\% \text{CF}_3\text{COOH}$ in H_2O 75/25 v/v, t_R = 7.12 min). MS ESI⁺ m/z 604.9 (M^+). Anal. (C,H,N).

3-Ethyl-2-[3-(3-ethyl-5-propyloxy-1,3-benzothiazol-2(3H)-ylidene)prop-1-en-1-yl]-1,3-benzothiazol-3-ium iodide (25). Reaction time 1 h; yield 51%. M.p. 240-242°C dec. (MeOH). ^1H -NMR (DMSO-*d*6) δ (ppm): 0.99 (t, 3H, $\text{CH}_3\text{CH}_2\text{CH}_2\text{O}$), 1.32 (t, 6H, $\text{CH}_3\text{CH}_2\text{N}$), 1.74 (m, 2H, $\text{CH}_3\text{CH}_2\text{CH}_2\text{O}$), 3.98 (t, 2H, CH_2O), 4.34 (m, 4H, $\text{CH}_3\text{CH}_2\text{N}$), 6.57 (t, 2H, $\text{CH}=\text{CH}-\text{CH}$, $^3J_{\text{HH}} = 12.1\text{Hz}$), 6.96 (d, 1H), 7.27 (s, 1H), 7.35 (t, 1H), 7.52 (t, 1H), 7.62 – 7.70 (m, 2H), 7.82 (d, 1H), 7.91 (d, 1H) (Btz, $\text{CH}=\text{CH}-\text{CH}$); ^{13}C -NMR (DMSO-*d*6) δ (ppm): 10.4, 12.6, 12.7, 41.4, 41.5, 69.8, 98.1, 99.0, 112.9, 130.1, 116.1, 123.0, 123.7, 124.9, 125.0, 128.0, 140.7, 142.0, 145.6, 159.4, 163.4, 165.1. PHPLC = 100% (mobile phase: $\text{CH}_3\text{CN}/0.1\% \text{CF}_3\text{COOH}$ in H_2O 70/30 v/v, t_R = 12.3 min). MS ESI⁺ m/z 423.1 (M^+). Anal. (C,H,N).

4.2. Activation of sGC

1×10^6 Human cells hCMEC/D3 were cultured in 6-well plates coated with 150 $\mu\text{g}/\text{mL}$ rat collagen type I, in EBM-2 basal medium (Lonza), supplemented with 1% v/v penicillin-streptomycin, 5% v/v fetal bovine serum, 1.4 μM hydrocortisone, 5 $\mu\text{g}/\text{mL}$ ascorbic acid, 1% v/v

chemically-defined lipid concentrate (Invitrogen), 10 mM Hepes, 1 ng/mL bFGF. Cells were maintained in a humidified atmosphere at 37°C, 5% CO₂. The medium was removed and replaced with 1 mL of Hepes-Ca²⁺ buffer (145 mM NaCl, 5 mM KCl, 1 mM MgSO₄, 10 mM Hepes sodium salt, 10 mM glucose, 1 mM CaCl₂, pH 7.4), containing the phosphodiesterase inhibitor 3-isobutyl-1-methylxanthine (IBMX) 1 mM. Cells were then incubated for 1h at 37°C with different concentrations of cyanine dyes (10 μM, 5 μM, 1 μM, 0.1 μM). SNP 1 mM was used as reference NO donor compound. At the end of the incubation period, the medium was removed from each well and 300 μL absolute ethanol were added to permeabilize the cells. Ethanol was evaporated completely under shaking. Samples were then dissolved in 250 μL of Tris-EDTA buffer (10 mM Tris, 1 mM EDTA, pH 8) and transferred into microcentrifuge tubes. The amount of cGMP was measured by the radio-immunoassay kit Cyclic GMP[3H] (Amersham Radiochemicals), following the manufacturer's instructions. The samples were counted by liquid scintillation. A titration curve was drawn through serial dilution of [3H]-cGMP. Results were expressed as pmol/10⁶ cells.

4.3. Thioflavin T assay for Aβ-peptide aggregation

To measure Aβ aggregation, a spectrofluorimetric method based on fluorescence emission of ThT was employed.^{33,34} The solution of ThT (3 μM) was prepared in phosphate buffer 50 mM, pH 6.0 and stored at 4°C. Samples for aggregation tests were prepared in phosphate-buffered saline (PBS 10 mM, NaCl 100 mM, pH 7.4) containing 2% 1,1,1,3,3,3-hexafluoro-2-propanol (HFIP) and 5% DMSO. In order to obtain batches of Aβ₄₀ free from preaggregates, commercial peptide (purity > 95%; Anaspec USA) was dissolved in 100% HFIP, dried under vacuum, and stored at -20°C.³⁴ Inhibitors were tested at different concentrations (30 μM peptide concentration), with incubation at room temperature for 2h. IC₅₀ values were determined by testing in triplicate 5 to 7 concentrations of all synthesized compounds, in at least three independent experiments. Aβ₄₂ (rPeptide, USA) aggregates were obtained by incubating the monomeric peptides for 5 days in the presence of 150 mM NaCl, at 37°C. To evaluate anti-aggregation activity, increasing concentrations of different compounds, or of their respective vehicles, were added during the incubation period. Compounds were solubilized in ethanol and diluted in aggregation buffer. The final concentration of vehicle was 0.5%. Fluorimetric measures were taken in 96-well microplates with a Perkin-Elmer spectrofluorimeter (Victor 4X

Multilabel Plate Reader). Parameters were set as follows: excitation, 450 nm; emission, 486 nm. Biological activity was determined as percentage of inhibitory activity V_i for each compound, calculated by the formula

$$V_i = 100 - \{[(F_i - F_b)/F_0] \times 100\}$$

where F_i is the fluorescence value of the sample, F_b its blank value, and F_0 the fluorescence value for free aggregation of a sample of $A\beta_{40}$ incubated in the absence of inhibitors. For the most active inhibitors, IC_{50} values could be calculated by nonlinear regression analysis (GraphPad Prism 5.0 software). For less active compounds, the percentage \pm SE of aggregation inhibition at 100 μ M was calculated.

The interference of cyanines in the formation of the fluorescent adduct between ThT and amyloid aggregates was also evaluated in a separate series of experiments. Samples for aggregation tests were prepared as described above and fluorescence intensity was measured after adding to amyloid aggregates ThT alone or together with either compounds **21** (20 μ M) or **22** (10 μ M) at the concentration that induced the maximum effect in inhibition experiments. No modification of the ThT fluorescence emission intensity was observed.

4.4. Tau aggregation in the presence of test compounds

The cDNA of the 441-amino acid tau isoform (2N4R), cloned in the pRK172 bacterial expression vector, was expressed in *Escherichia coli* BL21 (DE3 Novagen, Merck KGaA, Darmstadt, Germany) and purified as described elsewhere.^{51,52} Protease inhibitors were added and tau protein concentrations determined by densitometric analysis of Coomassie blue-stained sodium dodecyl sulphate polyacrylamide gels.

Tau protein (8 μ M) was incubated at 37°C in the presence of heparin (300 μ g/mL) (Sigma-Aldrich average MW 9.000 to 12.000 Daltons) in 35 mM MES buffer pH 7.4 and 1 mM DTT, alone or co-incubated with compounds **1**, **18**, **21**, **22**, or **24**, added at 1 μ M concentration. Staining and ultrastructural properties of protein aggregates were determined after 2 and 5 days of incubation as described elsewhere.⁵²

Briefly, at each time point 8 μ L aliquots were applied on Formvar-Carbon 200 mesh nickel grids for 5 min, negatively stained with super-saturated uranyl acetate aqueous solution, and observed under the electron microscope (EM109 ZeissOberkochen, Germany) operating at 80 KV at a standard magnification, calibrated with an appropriate grid. At the same time points, 10 μ L aliquots of peptide suspensions were air-dried on poly-L-lysine-coated slides (Bio-Optica) stained with the amyloid-binding dye Congo Red, and viewed under polarized light (Nikon Eclipse E-800 microscope). Morphological ultrastructural characteristics of aggregates – i.e. the presence and relative amount of amorphous materials, fibrils, protofibrils, and oligomers - were evaluated at 30,000 standard magnification.

4.5. Preparation of A β ₄₂ solutions for long-term potentiation recordings

Freeze-dried purified A β ₄₂ was purchased from AnaSpec and prepared as described elsewhere following standard procedures.^{39,41,42,53-55} Briefly, peptide was diluted to 1 mM in 1,1,1,3,3,3,-hexafluoro-2-propanol to disassemble preformed aggregates, and stored as dry films at 20°C until use. The films were dissolved at 1 mM in DMSO, sonicated for 10 min, diluted to 100 μ M in cold PBS, and incubated for 12–18 h at 4°C to promote protein oligomerization. The final working concentration (200 nM) was obtained by diluting the 100 μ M A β ₄₂ in extracellular solutions (for ACSF salt composition, see below). The same amount of DMSO/PBS contained in A β ₄₂ solutions was used as vehicle.

4.6. Long-term potentiation recordings

All animal procedures were approved by the Ethics Committee of the Catholic University, Rome, and complied with Italian Ministry of Health guidelines, with Italian laws (Legislative decree 116/1992), and with European Union guidelines on animal research (No. 86/609/EEC). Electrophysiological experiments were performed on 30-day-old male C57BL/6 mice, as described elsewhere.^{41,42,56} Animals were anesthetized with isoflurane and decapitated. The brains were rapidly removed and placed in ice-cold cutting solution containing the following: 124 mM NaCl, 3.2 mM KCl, 1 mM NaH₂PO₄, 2 mM MgCl₂, 1 mM CaCl₂, 26 mM NaHCO₃, 10 mM glucose, 2 mM Na-pyruvate, and 0.6 mM ascorbic acid, pH 7.4, 95% O₂/5% CO₂. Hippocampal slices (400 μ m thick) were cut on a vibratome (VT1000S; Leica Microsystems) and immediately transferred to an incubation chamber filled with ACSF

containing the following: 124 mM NaCl, 3.2 mM KCl, 1 mM NaH₂PO₄, 1 mM MgCl₂, 2 mM CaCl₂, 26 mM NaHCO₃, and 10 mM glucose, pH 7.4, 95% O₂/5% CO₂. Slices were allowed to recover at 32°C for 1 h before being equilibrated at room temperature. For electrophysiological recordings, slices were transferred to a submerged recording chamber constantly perfused with heated ACSF (32°C) and bubbled with 95% O₂/5% CO₂. For extracellular recordings of field excitatory synaptic potentials (fEPSP) at CA3-CA1 synapses of the hippocampus, the Schaffer collateral fibers were stimulated with a bipolar tungsten electrode (Warner Instruments). Recordings were made in the CA1 stratum radiatum using a glass electrode filled with ACSF (tip resistance 2–4 MΩ) and connected to a MultiClamp 700A amplifier (Molecular Devices, Sunnyvale, CA, USA). A Digidata 1440 Series interface and pClamp 10 software (Molecular Devices) were used for data acquisition and stimulation protocols. Data were filtered at 1 kHz, digitized at 10 kHz, and analyzed on- and off-line. Hippocampal subfields and electrode positions were identified with the aid of 4× and 40× water immersion objectives on an upright microscope equipped with differential interference contrast optics under infrared illumination (BX51WI; Olympus, Tokyo, Japan) and video observation (C3077-71 CCD camera; Hamamatsu Photonics, Japan). The stimulation intensity that produced one-third of the maximal response was used for the test pulses, and the LTP-induction protocol consisted of four trains of 50 stimuli at 100 Hz repeated every 20 s (high frequency stimulation paradigm, HFS). The magnitude of LTP was measured for 60 min after HFS and expressed as a percentage of baseline fEPSP peak amplitude. The mean values observed during the last 5 min of pre-HFS recordings were taken as baseline at 100%. For the experiments, 40 μL of Aβ₄₂ from 100 μM stock solution and 8 μL each of compounds **1**, **21** or **22** from 5 mM stock solutions, were mixed and diluted to a final volume of 20 ml, corresponding to a final Aβ₄₂ concentration of 200 nM, and to a final concentration of compound **1**, **21** or **22** of 2 μM. The diluted mixture was then pre-incubated for 30 min and then applied to brain slices for 20 min before LTP induction. Statistical analysis in all electrophysiological experiments (Student's unpaired t-test) was performed with SYSTAT 10.2 (Statcom).

Supplementary Information available. Elemental analysis for the final compounds, cytotoxicity assay, semiquantitative evaluation of tau protein aggregation inhibition.

Acknowledgment. This work was supported by grants from the University of Turin (Ricerca Locale ex-60% 2012 and 2013) and the Italian Ministry of Health (grant RF2009-1473239).

REFERENCES

1. Alzheimer's disease international: world Alzheimer report **2014**; London (UK).
2. Alzheimer disease and dementia; Alzheimer's association. www.alz.org (accessed Dec 15, **2014**).
3. Kalaria, R.N.; Hedera, P. *Neuroreport* **1995**, *6*, 477.
4. Palmer, A.M. *Trends Pharmacol. Sci.* **2011**, *32*, 141.
5. Gorevic, P.D.; Goni, F.; Ponestel, B.; Alvarez, F.; Peress, N. S.; Frangione, B. *J. Neuropat. Exp. Neur.* **1986**, *45*, 647.
6. Hamley, I.W. *Chem. Rev.* **2012**, *112*, 5147.
7. Bulic, B.; Pickhardt, M.; Schmidt, B.E.; Mandelkow, M.; Waldmann, H.; Mandelkow, E. *Angew. Chem. Int. Edit.* **2009**, *48*, 1741 and references therein.
8. Estrada, L.D.; Soto, C. *Curr. Top. Med. Chem.* **2007**, *7*, 115 and references therein.
9. Ballatore, C.; Lee, V.M.Y.; Trojanowski, J.Q. *Nat. Rev. Neurosci.* **2007**, *8*, 663.
10. Nunomura, A.; Castellani, R.J.; Zhu, X.W.; Moreira, P.I.; Perry, G.; Smith, M.A. *J. Neuropat. Exp. Neur.* **2006**, *65*, 631 and references therein.
11. Taniguchi, S.; Suzuki, N.; Masuda, M.; Hisanaga, S.; Iwatsubo, T.; Goedert, M.; Hasegawa, M. *J. Biol. Chem.* **2005**, *280*, 7614 and references therein.
12. Chang, E.; Congdon, E.E.; Honson, N.S.; Duff, K.E.; Kuret, J. *J. Med. Chem.* **2009**, *52*, 3539.
13. Necula, M.; Kaye, R.; Milton, S.; Glabe, C.G. *J. Biol. Chem.* **2007**, *282*, 10311.
14. Schneider, L.S.; Mangialasche, F.; Andreasen, N.; Feldman, H.; Giacobini, E.; Jones, R.; Mantua, V.; Mecocci, P.; Pani, L.; Winblad, B.; Kivipelto, M. *J. Intern. Med.* **2014**, *275*, 251.
15. Kerwin, J.F.; Heller, M. *Med. Res. Rev.* **1994**, *14*, 23.
16. Moncada, S.; Higgs, E.A. *Brit. J. Pharmacol.* **2006**, *147* (Suppl. 1), S193.
17. Jin, R.C.; Loscalzo, J. *J. Blood Med.* **2010**, *1*, 147.
18. Esplugues, J.V. *Brit. J. Pharmacol.* **2002**, *135*, 1079.

19. Austin, S.A.; Santhanam, A.V.; Katusic, Z.S. *Circ. Res.* **2010**, *107*, 1498.
20. Hardingham, N.; Dachtler, J.; Fox, K. *Front. Cell. Neurosci.* **2013**, *7*, 1.
21. Thatcher, G.R.J.; Bennett, B.M.; Reynolds, J.N. *Cur. Alzheimer Res.* **2005**, *2*, 171.
22. Schiefer, I.T.; VandeVrede, L.; Fa, M.; Arancio, O.; Thatcher, G.R.J. *J. Med. Chem.* **2012**, *55*, 3076.
23. Qjn, Z.; Luo, J.; VandeVrede, L.; Tavassoli, E.; Fa, M.; Teich, A.F.; Arancio, O.; Thatcher, G.R.J. *J. Med. Chem.* **2012**, *55*, 6784.
24. Chen, Y.; Sun, J.; Fang, L.; Liu, M.; Peng, S.; Liao, H.; Lehmann, J.; Zhang, Y. *J. Med. Chem.* **2012**, *55*, 4309.
25. a) Gasco, A.; Boschi, D.; Chegaev, K.; Cena, C.; Di Stilo, A.; Fruttero, F.; Lazzarato, L.; Rolando, B.; Tosco, P. *Pure Appl. Chem.* **2008**, *80*, 1693; b) Chegaev, K.; Riganti, C.; Lazzarato, L.; Rolando, B.; Guglielmo, S.; Campia, I.; Fruttero, R.; Bosia, A.; Gasco, A. *ACS Med. Chem. Lett.* **2011**, *2*, 494; c) Lazzarato, L.; Chegaev, K.; Marini, E.; Rolando, B.; Borretto, E.; Guglielmo, S.; Joseph, S.; Di Stilo, A.; Fruttero, R.; Gasco, A. *J. Med. Chem.* **2011**, *54*, 5478.
26. Bliss, T.V.; Collingridge, G.L. *Nature* **1993**, *361*, 31.
27. Nabavi, S.; Fox, R.; Proulx, C.D.; Lin, J.Y.; Tsien, R.Y.; Malinow, R. *Nature* **2014**, *511*, 348.
28. Sorba, G.; Ermondi, R.; Fruttero, U.; Galli, A.; Gasco A. *J. Heterocyclic Chem.* **1996**, *33*, 327.
29. Mason, S.J.; Hake, J.L.; Nairne, J.; Cummins, W.J.; Balasubramanian, S. *J. Org. Chem.* **2005**, *70*, 2939.
30. Thatcher, G.R.J.; Bennett, B.M.; Reynolds, J.N. *Cur. Alzheimer Res.* **2006**, *3*, 237 and references therein.
31. Gasco, A.; Schoenafinger, K. The NO-releasing heterocycles in *Nitric Oxide donors*; Wang P. G., Cai, T. B., Taniguchi, N., Eds.; Wiley-VCH: Weinheim, **2005**, 131.
32. Barrow, C.J.; Yasuda, A.; Kenny, P.Y.; Zagorski, M.G. *J. Mol. Biol.* **1992**, *225*, 1075.
33. LeVine, H.III. *Prot. Sci.* **1993**, *2*, 404.
34. Cellamare, S.; Stefanachi, A.; Stolfa, D.A.; Basile, T.; Catto, M.; Campagna, F.; Sotelo, E.; Acquafredda, P.; Carotti, A. *Bioorg. Med. Chem.* **2008**, *16*, 4810.

35. Volkova, K.D.; Kovalska, V.B.; Balanda, A.O.; Vermeij, R.J.; Subramaniam, V.; Slominskii, Y.L.; Yarmoluk, S.M. *J. Biochem. Biophys. Methods* **2007**, *70*, 727.
36. Duff, K.; Kuret, J.; Congdon, E.E. *Cur. Alzheimer Res.* **2010**, *7*, 235.
37. Puchtler H.; Sweat F.; Levine M. *J. Histochem. Cytochem.* **1962**, *10*, 355.
38. Malenka, R.C.; Malinow, R. *Nature* **2011**, *469*, 44.
39. Attar, A.; Ripoli, C.; Riccardi, E.; Maiti, P.; Li Puma, D.D.; Liu, T.; Hayes, J.; Jones, M.R.; Lichti-Kaiser, K.; Yang, F.; Gale, G.D.; Tseng, C.H.; Tan, M.; Xie, C.W.; Straudinger, J.L.; Klärner, F.G.; Schrader, T.; Frautschy, S.A.; Grassi, C.; Bitan, G. *Brain* **2012**, *135*, 3735.
40. Li, S.; Jin, M.; Zhang, D.; Yang, T.; Koeglsperger, T.; Fu, H.; Selkoe, D.J. *Neuron* **2013**, *77*, 929.
41. Ripoli, C.; Piacentini, R.; Riccardi, E.; Leone, L.; Li Puma, D.D.; Bitan, G.; Grassi, C. *Neurobiol. Aging* **2013**, *34*, 1032.
42. Ripoli, C.; Cocco, S.; Li Puma, D.D.; Piacentini, R.; Mastrodonato, A.; Scala, F.; Puzzo, D.; D'Ascenzo, M.; Grassi, C. *J. Neurosci.* **2014**, *34*, 12893.
43. Shichun, T.; Shu-ichi, O.; Stuart, A.L.; Huaxi, X. *Mol. Neurodegener.* **2014**, *9*, 48.
44. Selkoe, D.J. *Science* **2002**, *298*, 789.
45. Smith, D.L.; Pozueta, J.; Gong, B.; Arancio, O.; Shelanski, M. *Proc. Natl. Acad. Sci., USA*, **2009**, *106*, 16877.
46. Koral, M.; Leifer, A.; Bonis, D.; Collins, M.; Dougherty, P.; Fusco, A.J.; Luvalleet, J.E. *J. Chem. Eng. Data* **1965**, *10*, 67.
47. Biava, M.; Porretta, G.C.; Poce, G.; Battilocchio, C.; Alfonso, S.; Rovini, M.; Valenti, S.; Giorgi, G.; Calderone, V.; Martelli, A.; Testai, L.; Sautebin, L.; Rossi, A.; Papa, G.; Ghelardini, C.; Mannelli, L.C.; Giordani, A.; Anzellotti, P.; Bruno, A.; Patrignani, P.; Anzini, M. *J. Med. Chem.* **2011**, *54*, 7759.
48. Calvino, R.; Mortarini, V.; Gasco, A.; Sanfilippo, A.; Ricciardi, M.L. *Eur. J. Med. Chem.* **1980**, *15*, 485.
49. Di Stilo, A.; Visentin, S.; Cena, C.; Gasco, A.M.; Ermondi, G.; Gasco, A. *J. Med. Chem.* **1998**, *41*, 5393.
50. Farrar, W.V. *J. Chem. Soc.* **1964**, 904.
51. Rossi, G.; Bastone, A.; Piccoli, E.; Mazzoleni, G.; Morbin, M.; Uggetti, A.; Giaccone, G.; Sperber, S.; Beeg, M.; Salmons, M.; Tagliavini, F. *Neurobiol. Aging* **2012**, *33*, 834.

52. Rossi, G.; Bastone, A.; Piccoli, E.; Morbin, M.; Mazzoleni, G.; Fugnanesi, V.; Beeg, M.; Del Favero, E.; Cantù, L.; Motta, S.; Salsano, E.; Pareyson, D.; Erbetta, A.; Elia, A.E.; Del Sorbo, F.; Silani, V.; Morelli, C.; Salmona, M.; Tagliavini, F. *Neurobiol. Aging* **2014**, *35*(2), 408.
53. Piacentini, R.; Ripoli, C.; Leone, L.; Misiti, F.; Clementi, M.E.; D'Ascenzo, M.; Giardina, B.; Azzena, G.B.; Grassi, C. *J. Neurochem.* **2008**, *107*, 1070.
54. De Chiara, G.; Marcocci, M.E.; Civitelli, L.; Argnani, R.; Piacentini, R.; Ripoli, C.; Manservigi, R.; Grassi, C.; Garaci, E.; Palamara, A.T. *PLoSOne* **2010**, *5*, e13989.
55. Maiti, P.; Piacentini, R.; Ripoli, C.; Grassi, C.; Bitan, G. *Biochem J.* **2011**, *433*, 323.
56. Fusco, S.; Ripoli, C.; Podda, M.V.; Chiatamone Ranieri, S.; Leone, L.; Toietta, G.; McBurney, M.W.; Schütz, G.; Riccio, A.; Grassi, C.; Galeotti, T.; Pani, G. *Proc. Natl. Acad. Sci., USA*, **2011**, *109*, 621.